NRC Publications Archive
Archives des publications du CNRC

Chemical vapor generation characteristics of transition and noble metals reacting with tetrahydroborate (III)
Feng, Y. L.; Sturgeon, R.; Lam, J.

NRC Publications Record / Notice d'Archives des publications de CNRC:
https://nrc-publications.canada.ca/eng/view/object/?id=c99b777c-6bf0-4057-8ef4-00255ac5d928
https://publications-cnrc.canada.ca/fra/voir/objet/?id=c99b777c-6bf0-4057-8ef4-00255ac5d928

National Research Council Canada   Conseil national de recherches Canada

Canada

Chemical vapor generation characteristics of transition and noble metals reacting with tetrahydroborate(III)†

Yong-Lai Feng,[b] **Ralph E. Sturgeon***[a] **and Joseph W. Lam**[a]

[a]*Institute for National Measurement Standards, National Research Council of Canada, Ottawa, Canada K1A 0R9*
[b]*Chemistry Research Division, Health Canada, Tunney's Pasture, Ottawa, Canada K1A 0L2*

The vapor generation characteristics of several transition and noble metals arising from reduction of their aquo-ions by tetrahydroborate(III) are presented. A modified parallel path Burgener Teflon nebulizer interfaced to an ICP-MS for detection was used to examine the effects of experimental variables. The influence of both hydrochloric and nitric acid as well as the nature of the surface exposed to the nascent species is of paramount importance to the overall efficiency of the generation process. Both glass and Ryton double pass spray chambers were examined, the latter providing superior performance with respect to sensitivity as well as memory effects. Data were presented for the generation of vapor phase species of Rh, Pd, Au and Cu that can be collected in a weakly acidic medium for subsequent release as a gaseous product.

Introduction

The generation of gaseous analytes and their introduction into atomic spectrometric sources offers several significant advantages over conventional pneumatic nebulization of solution samples. These include elimination of the need for a nebulizer, enhancement of analyte transport efficiency, the presentation of a homogeneous vapor to the plasma, and removal of the matrix to minimize interferences. Historically, this research has concentrated on the classic hydride-forming elements, *viz.*, Se, As, Sb, Te, Bi, Ge and Sn. In the case of transition metals and noble elements, on the other hand, generation of volatile chlorides, fluorides, β-diketonates, dithiocarbamates and carbonyls has usually been pursued.

Hydride generation is well known for the convenience of its reaction between tetrahydroborate(III) reductant and target analytes in an acidified sample solution. Recently, the scope of this technique has been expanded to include several transition and noble elements.[1–20] Sanz-Medel *et al.*[8] reported on the generation of a volatile species of Cd following reduction of Cd(II) with sodium tetrahydroborate(III) in aqueous solutions containing vesicles of didodecyldimethylammonium bromide. Sturgeon *et al.*[1–7,20] published a series of papers on the vapor generation of Cu, Au, Ag, Zn, Rh, Pd, In, Ti, Ir, Pt, Mn, Hg, Tl, Pb and Cd with sodium tetrahydroborate(III). Pohl and Zyrnicki[10–12] presented evidence for enhanced sample introduction efficiencies for Co, Cr, Fe and Ni, achieved following reaction of solutions of these metals with tetrahydroborate(III) when using a Meinhard nebuliser. They also concluded that vapor generation of Os, Rh and Ru occurred following reduction by tetrahydroborate(III). Silver, Cd, Au, Co, Cu, Ni, Sn and Zn have also been reported by Duan *et al.*[13] to be amenable to vapor generation by reaction with tetrahydroborate(III). Wang *et al.*[16] studied the generation of Cd and Cu species using a moving bed reduction generator. Matousek *et al.*[18] investigated reduction of Ag using tetrahydroborate(III) but were not able to definitively identify the vapor phase species produced, despite enhanced transport efficiency to the detection system. Du and Xu[19] reported that Au yields a volatile

species during reduction by tetrahydroborate(III) in an acidified solution in the presence of sodium diethyldithiocarbamate.

This study focuses on the general characteristics of vapor generation when applied to transition and noble metals and attempts to provide some insight into this reaction. This is the first report detailing such fundamental studies relating to the generation of volatile species of transition and noble metals resulting from the continuous merging of an acidified analyte solution with a solution of sodium tetrahydroborate(III). A modified parallel path Burgener nebulizer was used for this purpose.

Experimental

Instrumentation

A PerkinElmer SCIEX (Concord, Ontario, Canada) Model ELAN 5000 operating under conditions summarized in Table 1 was used. A modified Burgener parallel path nebulizer was used for vapor generation, as described earlier.[4] To minimize aerosol formation, the aerosol gas channel (herein designated as the "shear gas") was concentric with both the sample and tetrahydroborate(III) solution channels. This arrangement also permitted control over the reaction time between the acidified sample solution and the tetrahydroborate(III).[6]

Both Ryton [poly(*p*-phenylene) sulfide] and glass double-pass

Table 1 Operating parameters for vapor generation with ICP-MS detection

Rf power	1000 W
Plasma gas flow rate	15 L min^{-1}
Intermediate gas flow rate	1.1 L min^{-1}
Shear gas flow rate	0.4 L min^{-1}
Make-up gas flow rate	0.45 L min^{-1}
Scanning mode	Peak hop
Replicate time	100 ms
Dwell time	100 ms
Sweeps/reading	1
Reading/replicate	Variable
Points/spectral peak	1
Resolution	Normal
Skimmer and sampling cone	Nickel
Sample flow rate	1.1 mL min^{-1}
NaBH$_4$ flow rate	1.1 mL min^{-1}

spray chambers were investigated. The nebulizer was mated to the spray chamber with the use of a standard commercial push-fit Teflon end cap. The glass spray chamber was fabricated in-house and was of the same dimensions as that of a commercial PerkinElmer–Sciex double-pass Ryton chamber. It was designed to permit substitutions of its inner (first pass) glass tube with ones of variable dimensions and of different material (*i.e.*, Ryton). For this purpose, the inner glass tube was mounted in place with the use of a Teflon bung. A commercial Ryton double-pass spray chamber was similarly modified in that its center tube was also mounted in place with a Teflon bung to permit both the standard Ryton inner tube as well as various glass tubes to be used with the spray chamber. A "make-up" flow of Ar gas, maintained with a mass flow controller, was merged with the outlet stream from the spray chamber to permit optimization of a carrier gas flow independent of the total gas flow entering the plasma.

Sample and reductant streams were introduced either in a continuous manner at a flow rate of 1.1 mL min^{-1} each, using a four channel 12 roller Minipuls 2 peristaltic pump (Gilson, Middleton, WI, USA), or the sample was added discretely, injected as an 80 μL volume using a loop inserted into the acidified sample steam. For this purpose, a flow injection manifold fitted with a manual metal free injection valve for merging the loop contents with a continuous stream of reductant was used.

Reagents

Stock solutions (1000 μg mL^{-1} of As(III), Se(IV), Sb(III), Cu(II), Ag(I), Au(III), Zn(II), Cd(II), Ni(II), Pd(II), Pt(II), Hg(II), Ti(III), Rh(II), Ir(II), Co(II), Cr(III), Fe(III), Mn(II), In(II), Tl(II), Mg(II) and Pd(II)) were obtained from SCP Science (Montreal, PQ, Canada). Working standards of lower concentration were prepared by dilution of the stocks using 18 MΩ cm deionized, reverse osmosis water (DIW) obtained from a mixed-bed ion-exchange system (NanoPure, Model D4744, Barnstead/Thermolyne, Dubuque, IA, USA). High-purity sub-boiling distilled HCl and HNO$_3$ were prepared in-house and used for acidification of the working standards. A 1% (*m/v*) solution of sodium tetrahydroborate(III) in 0.001 M NaOH was prepared daily, or more frequently if required. Both reagents were purchased from Alfa Aesar (Ward Hill, MA, USA). Dimethyldichlorosiloxane was purchased from Pierce Chemical Co. (Rockford, IL, USA).

All solutions were prepared in a clean room providing a class 100 working environment and all glassware was soaked for 24 h

in 1 M HNO$_3$ and rinsed with DIW before use. Argon gas was obtained from Praxair (Mississauga, ON, Canada).

Procedures

Once the argon plasma was stabilized, the vapor generator was brought on-line. A steady-state signal for each analyte was obtained, using a 100 ng mL^{-1} feed solution, and the instrument peaked for maximum response. A number of variables were optimized, including the effect of total plasma gas flow rate, shear gas flow rate, make-up gas flow rate, analyte and reductant solution flow rates, acid and reductant concentration. Data were collected and manipulated using MS Excel and in-house software. When possible, at least two isotopes were used for signal measurement of each element. A shear gas flow rate of 0.4 L min^{-1} was optimized for the production/separation of volatile species from the merged solutions immediately at the generator tip. This differs substantially from typical conditions used for conventional pneumatic nebulization when maximum aerosol generation efficiency is desired. Owing to the design and operation of the generator, almost no aerosol was introduced into the plasma using the conditions noted above, as evidenced by the small signals arising at *m/z* 75 and 77 in a hydrochloric acid medium (which would normally give rise to intense signals due to ^{40}Ar^{35}Cl and ^{40}Ar^{37}Cl). In order to verify that the signals observed were actually due to the analyte element, response was compared to that obtained during introduction of acidified blank solutions.

In the "collection mode",[20] the nebulizer was inserted through the side-wall of a 3.5 cm id glass gas sparger containing approximately 10 ml of DIW.[20] The tip of the nebulizer protruded through a port fabricated in the wall of the vessel (sealed with Teflon tape) about 5 mm from the bottom and such that a 5 mm head of water remained above the tip. The outlet from the sparger was directed to the plasma torch for introduction of any volatile forms of the metal so produced. An external mass flow controller was used to regulate the Ar flow rate through a three-way valve fitted to the sparger, thereby ensuring a constant optimized gas flow to the plasma under all conditions. This arrangement is illustrated in Fig. 1.

Results and discussion

In contrast to the conventional hydride-forming elements, such as As and Se, transition and noble metals require rapid separation of the volatile species from the reaction medium, suggesting the product is very unstable in the liquid phase.[1,13]
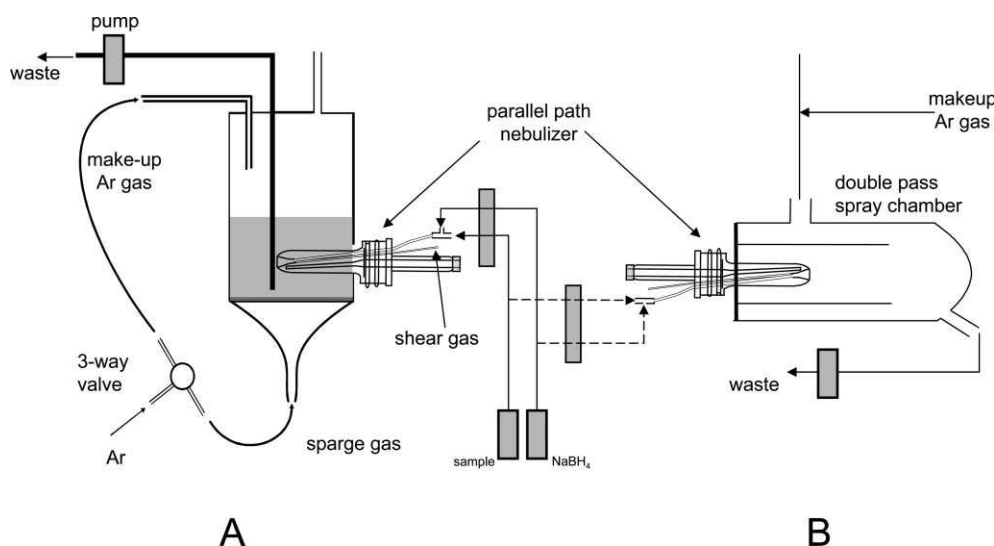

Fig. 1 Schematic of the vapor collection (A) and generation (B) system.

This leads to relatively poor overall generation efficiencies, as noted earlier.[4] Rapid gas–liquid separation was thus attempted during all phases of this study. Iridium, Pd, Ag, Rh, Co and Cu were selected as representative elements of those studied to serve as illustrative examples for discussion of the various phenomena highlighted below.

Effect of surface material

The nature of the spray chamber surface affects the efficiency of the vapor generation process for transition and noble elements. As noted earlier, both a Ryton and a glass double-pass spray chamber were mated to the Burgener nebulizer in an effort to discern the effects of the physicochemical properties of the surfaces of these materials in contact with the generation medium. Rather surprising results were obtained, as illustrated in Figs. 2 (a–c), which show typical response from Ir, Ag and Pd. The signals displayed show the effect on response of generation of the volatile analyte in varying concentrations of either HCl or HNO_3 used for continuously merging the acidified sample stream with a 1% (m/v) solution of $NaBH_4$ reductant. Between each sample introduction, the system was 'washed' out with the corresponding acid blank. The nature of the spray chamber surface affects not only the peak intensity, but its shape as well. In the presence of a Ryton surface, no wash in, wash out, drift or memory effects are evident for any of these elements using either acid as the generation medium. By contrast, when a glass spray chamber is used, signal intensities for Ir in both acids are attenuated almost 10-fold and a serious memory effect or wash out problem occurs for Ag and Pd [as well as Au, amongst other elements studied (not shown)]. It is clear that an element specific generation surface interaction is operative and underscores the assumption that

generation of these volatile analyte species appears to proceed *via* a two-step mechanism, wherein the surface may play a role in stabilizing an intermediate atomic species.[20] A Ryton spray chamber provids superior performance compared with a glass one, irrespective of the type of acid used.

An earlier report by Duan *et al.*[13] suggested that the use of thiourea in HCl may serve to alleviate memory effects, but all such attempts to implement this with the present system proved futile. Fortunately, use of a Ryton based system completely obviated this need.

Effect of acid generation medium

Both nitric and hydrochloric acids were investigated for their effects on the response in both spray chamber systems and, in general, both acids proved amenable for use. The specific effects of these acids could be discerned in the well-behaved Ryton system. In the case of Ir (Fig. 2(a)), both HCl and HNO_3 exhibited similar effects, *i.e.*, an initial rise in signal intensity as the acid concentration in the sample stream increased from 0.05 to 0.1 M, followed by decreased response with further increases in concentration of either acid. No significant difference in sensitivity was noted when using either acid. It is clear from Fig. 2(b) that, for Ag (and Au, not shown), concentrations of HCl > 0.75 M suppressed signals and essentially eliminated them at 4 M, whereas HNO_3 could be used over a broad concentration range, with no significant deterioration in response even at 4 M. For Pd (Fig. 2(c)), a broad concentration range for both acids beyond 0.5 M was found optimal and even 2 M HCl could be tolerated. These observations again highlight the individual chemistries operative in these systems.

It is significant to note that the amount of aerosol formed should be expected to increase with acid concentration, due to
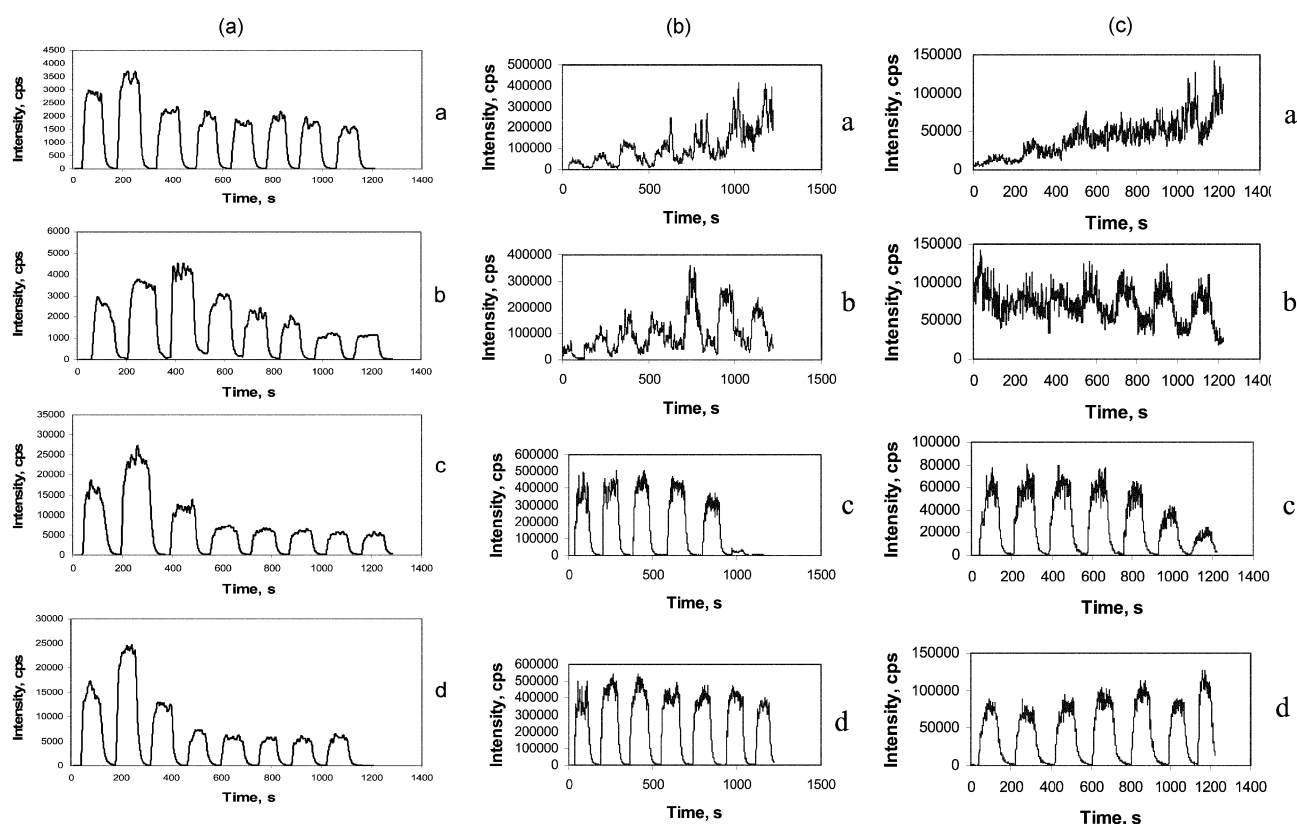
Fig. 2 Effect of acid concentration and spray chamber material on vapor generation of Ir, Ag and Pd using 1% (m/v) $NaBH_4$ in 0.001 M NaOH. Peak scans from left to right in each panel: 0.05, 0.10, 0.25, 0.50, 0.75, 1.0, 2.0, 4.0 M acid. (a) [Ir] = 200 ng mL^{-1}, m/z = 193. a, Nitric acid with glass spray chamber; b, hydrochloric acid with glass spray chamber; c, nitric acid with Ryton spray chamber; d, hydrochloric acid with Ryton spray chamber. (b) [Ag] = 100 ng mL^{-1}, m/z = 107. a, Hydrochloric acid with glass spray chamber; b, nitric acid with glass spray chamber; c, hydrochloric acid with Ryton spray chamber; d, nitric acid with Ryton spray chamber. (c) [Pd] = 200 ng mL^{-1}, m/z = 106. a, Hydrochloric acid with glass spray chamber; b, nitric acid with glass spray chamber; c, hydrochloric acid with Ryton spray chamber; d, nitric acid with Ryton spray chamber.

the enhanced intensity of hydrolysis of the tetrahydroborate(III) solution. This observation has also been noted earlier.[4] The existence of an optimal acid concentration in some cases and the decrease of analyte response with increasing acid concentration in others, support the conclusion that these species are transported to the torch in a form that is not associated with the aerosol phase. Further, the noticeable influence of the material of construction of the spray chamber on response again rules out a simple physical transport process. These conclusions were also consistent with the observations of performance for other elements in these systems.

The elements investigated were divided into approximately 4 groups, using criteria relating to memory effect, performance in glass *versus* Ryton and the effect of the acid generation medium. Such a division is reflected in the summary data presented in Table 2. In the first group appear elements that suffer from memory effects in a glass equipped system (note that no memory effects were encountered for any elements when a Ryton system was used) and have a response that is nearly independent of the type of acid used as the generation medium and for which the Ryton surface provides for a significantly better sensitivity. This group includes Cu, Pd, Ag, Au, Pt, Co, Ni, Rh and Tl. The second set comprises Ti, Mn, Ir and Zn, a group of elements free of memory effects, for which the Ryton surface continues to be significantly preferable with respect to sensitivity and for which generation appears to be essentially independent of the type of acid used. The third set, Cd, In, Hg and Pb, suffers no memory effects but performance is superior (by typically 5-fold) when the species are generated in a glass spray chamber. Additionally, response is somewhat sensitive to the type of acid used in the generation medium. The last group of elements comprises As, Se and Sb, which suffers no memory effects, enhanced performance when generated in a glass system and whose response is independent of the type of acid used in the generation medium.

Reductant effects

The concentration of tetrahydroborate(III) reagent is usually an important variable affecting vapor generation, not only for the conventional hydride-forming elements, but for transition and noble metals as well.[4] Most elements studied exhibit an optimum concentration of tetrahydroborate(III), as summarized by the data in Table 3. The exceptions are Tl, Cd, and Co, whose response continues to increase with reductant concentration. One noteworthy observation is that the tetrahydroborate(III) concentration not only affects signal intensity, but also its shape. Increasing concentrations of reductant give rise to large and spurious noise peaks. High concentrations of reductant give rise to an increase in the number and size of H_2 gas bubbles developed in the delivery line, which may be responsible for the increased noise as delivery of a smooth flow of reductant becomes practically impossible. A 1% (*m/v*) solution of the reductant was selected for further study in that a compromise is achieved between adequate signal intensity and shape.

Effect of shear gas

The shear gas flow rate affects the analyte phase separation efficiency. The shear gas in this system serves three functions: one is to ensure that the analyte and reductant solutions are well mixed following their confluence; another is to enhance the separation of the resultant volatile species from the liquid phase as quickly as possible by formation of an effluent stream having a large surface area/volume ratio; and finally, the shear gas aids in the transport of the analyte species to the plasma while minimizing its residence time in the spray chamber, thereby minimizing its decomposition. The apparent generation efficiency for most analytes increases with increased shear gas flow rate and reaches a maximum at approximately 0.4–0.5 L min^{-1}. Flow rates of 0.4 L min^{-1} for the shear gas and 0.45 L min^{-1} for the make-up gas were selected as a compromise between additional slight enhancements in signal intensity with increased shear gas flow rate and increased signals at *m/z* 75 and 77, which were indicative of aerosol carryover to the plasma, producing substantial loading by Na and Cl.

The shear gas flow rate has a significant impact on response as it influences analyte release and transport processes. Data presented in Table 4 show that a minimum flow rate is required to effect a rapid separation of the analyte vapor from the liquid

Table 2 Summary of optimized generation conditions

	HCl		HNO$_3$			
	Concentration/M	NR^a	Concentration/M	NR^a	Ryton/glass^b	Memory^c
^{65}Cu	0.25	0.93	0.25	1.0	1.6	Y
^{106}Pd	0.50	0.83	4.0	1.0	2.8	Y
^{107}Ag	0.50	0.88	0.50	1.0	5.7	Y
^{197}Au	0.75	0.72	1.0	1.0	4.4	Y
^{95}Pt	0.50	1.0	0.10	0.75	4.9	Y
^{59}Co	0.10	1.0	0.10	0.95	3.8	Y
^{60}Ni	0.25	0.83	0.05	1.0	4.6	Y
^{103}Rh	0.50	1.0	0.10	0.41	3.3	Y
^{205}Tl	0.05	1.0	0.10	0.66	4.1	Y
^{48}Ti	0.25	1.0	0.25	1.0	8.5	N
^{55}Mn	0.10	1.0	0.10	1.0	7.7	N
^{193}Ir	0.10	1.0	0.10	1.0	6.8	N
^{64}Zn	0.25	0.84	0.10	1.0	4.8	N
^{114}Cd	0.10^d	0.77	0.10^d	1.0	0.13	N
^{115}In	0.25^d	1.0	0.10^d	0.69	0.22	N
^{202}Hg	uniform^d	1.0	uniform^d	1.0	0.21	N
^{208}Pb	0.01^d	0.92	0.01^d	1.0	0.34	N
^{75}As	1^d	1.0	1.0^d	1.0	0.75	N
^{78}Se	1^d	1.0	1.0^d	1.0	0.37	N
^{121}Sb	0.50^d	1.0	0.50^d	1.0	0.59	N

^{a}Normalized response. ^{b}Ratio of net responses. ^{c}In a system fitted with a glass spray chamber. ^{d}In a glass spray chamber system.

Table 3 Effect of tetrahydroborate(III) concentration on normalized response with continuous generation in a Ryton system

	NaBH$_4$ (% m/v)					
	0.1	0.5	1.0	2.0	4.0	Optimum acid/(M)
^{65}Cu	0.03	0.29	1.0	0.59	0.31	HCl (0.25)
^{106}Pd	0.84	1.0	0.94	0.6	0.18	HNO$_3$ (0.5)
^{107}Ag	0.97	0.99	1.0	0.58	0.28	HNO$_3$ (0.5)
^{197}Au	0.57	0.95	1.0	0.94	0.44	HNO$_3$ (1.0)
^{195}Pt	0.42	0.61	1.0	0.74	0.81	HCl (0.5)
^{59}Co	0.004	0.15	0.75	0.93	1.0	HCl (0.1)
^{60}Ni	0.81	0.42	0.91	1.0	0.67	HNO$_3$ (0.05)
^{103}Rh	0.08	0.22	0.41	1.0	0.84	HCl (0.5)
^{205}Tl	0.072	0.10	0.17	0.31	1.0	HNO$_3$ (0.1)
^{48}Ti	0.35	0.75	0.78	1.0	0.83	HCl (0.25)
^{55}Mn	0.21	0.61	0.86	1.0	0.84	HCl (0.1)
^{193}Ir	0.27	0.10	0.98	0.77	0.49	HCl (0.1)
^{64}Zn	0.10	0.34	0.45	1.0	0.96	HNO$_3$ (0.25)
^{114}Cd	0.012	0.48	0.92	1.0	0.65	HCl (0.1)
^{115}In	0.35	0.61	0.82	0.92	1.0	HCl (0.1)
^{202}Hg	0.72	1.0	0.95	0.9	0.95	HCl (0.1)
^{208}Pb	1.0	0.75	0.48	0.25	0.17	HCl (0.01)

phase. Although an excessive flow rate could dilute the analyte concentration in the gas stream and lead to a decline in signal intensity, the total gas flow rate introduced into the central channel of the torch (*i.e.*, the sum of the shear gas and the make-up gas) was maintained constant (at 0.85 L min^{-1}) in all experiments so as to eliminate this effect.

Effect of mixing time

If the inner tube of the Burgener nebulizer is retracted, such that the acidic sample and reductant solutions have a longer time to interact before reaching the tip of the nebulizer and entering the spray chamber, the signal intensity typically decreases for all analytes (with the exception of the common hydride forming elements). Rapid separation of the analyte from the aqueous phase is required to achieve optimum signal response; a longer

**Table 4** Effect of shear gas flow rate on normalized response using a Ryton spray chamber

	L min^{-1}					
	0.2	0.3	0.4	0.5	0.6	0.7
^{65}Cu	0.61	0.84	0.87	0.98	1.0	0.89
^{106}Pd	0.60	0.93	1.0	0.96	0.79	0.71
^{107}Ag	0.53	0.81	0.93	1.0	0.97	0.95
^{197}Au	0.66	0.92	1.0	0.96	0.92	0.84
^{195}Pt	0.75	0.80	0.95	1.0	0.85	0.75
^{59}Co	0.57	0.74	0.80	0.87	1.0	0.91
^{60}Ni	0.59	0.77	0.82	0.91	1.0	0.91
^{103}Rh	0.73	0.96	1.0	0.93	1.0	1.0
^{205}Tl	0.58	0.83	0.92	0.96	1.0	1.0
^{48}Ti	0.46	0.70	0.88	1.0	0.90	0.82
^{55}Mn	0.63	0.83	0.88	1.0	1.0	0.93
^{193}Ir	0.49	0.71	0.77	0.81	1.0	1.0
^{64}Zn	0.50	0.80	1.0	1.0	0.76	0.67
^{114}Cd	0.32	0.44	0.74	0.82	0.97	1.0
^{115}In	0.63	0.75	0.80	1.0	0.90	0.8
^{202}Hg	0.56	0.71	0.79	0.85	0.96	1.0
^{208}Pb	0.44	0.71	0.94	1.0	1.0	0.94
^{75}As	0.43	0.66	0.76	0.77	0.91	1.0
^{78}Se	0.60	0.80	0.84	0.90	1.0	1.0
^{121}Sb	0.93	1.0	1.0	1.0	1.0	1.0

[a] Constant shear plus make-up gas flow of 0.85 L min^{-1} delivered to plasma; typical RSD is 10–15% for replicate signals; optimum acid type and concentration as identified in Table 2, 1% (m/v) NaBH$_4$.

reaction time or residence time in the aqueous phase provides more opportunity for additional reaction with the reductant, possibly resulting in formation of precipitates or other potential hydrolysis or reoxidation reactions, supporting ours' and others' earlier conclusions on the effect of this variable.[1,6,13,21] Enhanced mixing time also results in the appearance of black deposits on the inside of the reaction tube. If conventional batch approaches to vapor generation are attempted with these elements, no response is achieved.

Stability of volatile species

If the outlet from the spray chamber is directed through a column (2.5 cm id × 2.5 cm deep) of DIW, 0.5 M HCl or 0.5 M NaOH *via* a 4 mm id Teflon line before entering the ICP, some interesting results are obtained that can be compared to those reported for Cd and Hg,[20] as well as those for conventional hydride-forming elements. In contrast to Cd and Hg, signals from Ag, Au and other transition and noble metals are attenuated more than 85%, suggesting that the species are unstable and easily decomposed on passage through such a bubbler. However, once the nebulizer is itself submerged into the column of DIW to permit the generated species to directly enter this medium, as described earlier,[20] the analyte can be "collected" and subsequently stripped from this aqueous reservoir using a sparge gas and transported to the plasma, although with much decreased response compared with its direct passage to the plasma. Most significantly, collection or concentration of some analyte species can be accomplished in a weakly acidic medium, as evidenced by the proportional increase in the integrated signal intensity that can be achieved with increasing collection (generation) time prior to sparging the collection solution. This was evident for Rh, Pd, Au and Cu. Fig. 3 provides examples of this effect for vapor generation and collection of Rh and Pd. Generation/collection periods of 2, 4 and 8 min were investigated and consisted of the steady-state introduction of analyte and reductant streams to the nebulizer for these time periods while continuously purging the headspace above the DIW column with a 0.4 L min^{-1} flow of Ar to transport any available analyte to the plasma. Note that, during the generation process, there was no shear gas applied to the concentric flow at the nebulizer, hence no directed flow of gas through the water column (with the exception of that arising from any hydrogen resulting from the acid–borohydride reaction). Following this defined generation/collection period, sample introduction was ceased and the sparge gas sweeping the headspace was now directed through the aqueous solution to de-gas any dissolved (collected) analyte from the reservoir and transport it to the plasma.[20] While the headspace was being continuously swept with gas, monitoring of response revealed a continuous, but slow, increase in signal, representative of that fraction of the analyte species that did not "dissolve" in the aqueous phase or was being continuously and slowly stripped from it due to the evolution of hydrogen gas. With sparging of the solution, a transient response is generated, corresponding to the amount of analyte "collected" in the reservoir that had survived decomposition. Integration of the pulse intensity revealed a correlation between response and the generation/collection time, as shown in the insets to Figs. 3a and b. One possible explanation for this phenomenon is that the species produced are, in fact, nanoparticles of the reduced analyte that are sufficiently small as to be transported through the system in much the same manner as a gas.[22] Another possibility is that vapor phase species are indeed formed and are soluble (as a gas) to some extent in the water and can be concentrated for subsequent rapid release. It is self-evident that a linear relationship between the generation time and the integration of response over the entire signal registration period will be linear as this simply reflects a measure of the total amount of analyte delivered to the system. A linear
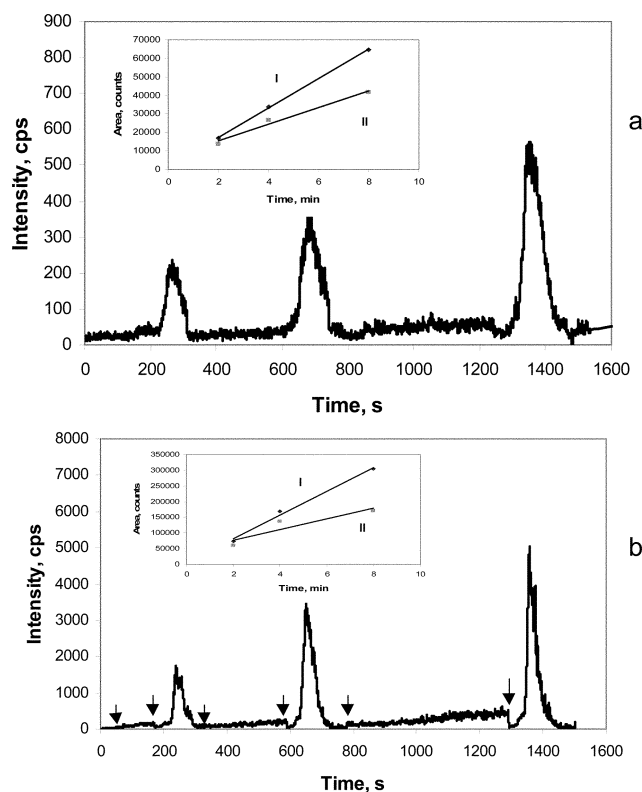
Fig. 3 Typical response arising from generation/collection of vapor species in a column of pH 5 (final) DIW with subsequent sparging of the "dissolved" analyte and its transport to the plasma for detection. Pairs of arrows represent points in time at which generation/collection commences or sparging of the solution begins. a, Generation/collection of 100 ng mL^{-1} Rh in 0.5 M HCl with 1% (m/v) NaBH$_4$ containing 0.001 M NaOH for 2, 4 and 8 min in a column of DIW using continuous delivery of reactants at 1.1 mL min^{-1} of both reagents, no shear gas flow is used. b, Generation/collection of 200 ng mL^{-1} Pd in 0.5 M HNO$_3$ with 1% (m/v) NaBH$_4$ containing 0.001 M NaOH for 2, 4 and 8 min in a column of DIW using continuous delivery of reactants at 1.1 mL min^{-1} of both reagents: no shear gas flow is used. Insets illustrate calibration curves prepared from the integrated counts (I) accumulated during the entire generation/collection/sparging process and (II) accumulated under only the sparging peak.

relationship is also depicted for the case when only the pulse (transient response) portion of the signal is integrated, reflecting a measure of the amount of analyte trapped in the solution. It is likely more accurate to describe this relationship as being non-linear because of the way the experiment was conducted. As the generation/collection time is increased, there is a proportionally longer time during which decomposition reactions within, and diffusion of the analyte from, the aqueous phase can occur. These processes lead to losses in response that increase with generation time. In hindsight, a more idealized approach would have been to vary the concentration of the analyte in the feed solution while maintaining the generation time constant, in which case the relationship between the transient response and the analyte concentration would be expected to be more linear than that obtained in these experiments. All other elements studied exhibited similar such "sparging peaks", but none produced a proportional relationship between their integrated intensity and collection time. Note that all signals were corrected for any intensity contribution from the processing of a blank.

Closer inspection of the data suggests that it may be possible to obtain an order of magnitude estimate of the efficiency of collection of the species in the DIW medium. Based on the sensitivity of measurement for direct transport of the analyte from the generator to the torch (i.e., 2×10^7 Hz ppm^{-1} for ^{103}Rh and 1.4×10^6 Hz ppm^{-1} for ^{106}Pd[4]), and the integrated response from each of the peaks corresponding to a 2 min
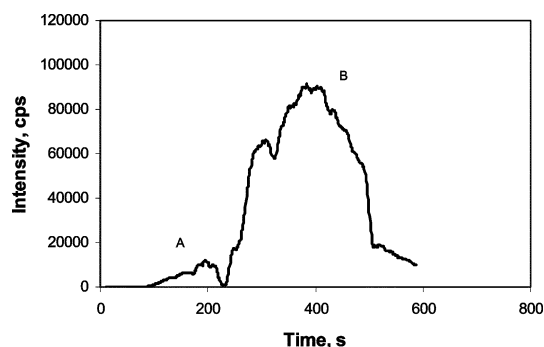
Fig. 4 Effect of shear gas flow rate on response from ^{106}Pd following generation of analyte by continuous merging of 1.1 mL min^{-1} flows of 200 ng mL^{-1} Pd in 0.5 M HNO$_3$ with a 1% (m/v) NaBH$_4$ solution containing 0.001 M NaOH in a system fitted with a Ryton spray chamber and directing the volatile product through a bubbler column of DIW. A, 0.1 L min^{-1}; B, 0.5 L min^{-1}.

generation period for 100 ppb Rh and 200 ppb Pd feed solutions (i.e., 14 500 counts for Rh and 57 400 counts for ^{106}Pd, cf. Fig. 3), an efficiency of 0.006% and 0.17% is calculated for the collection of Rh and Pd in the water column. These data do not account for the fact that decomposition of the species occurs immediately following their generation, and without knowledge of the half-life of the analyte in the medium it is impossible to estimate the true generation/capture efficiency. In any case, more than 99% of the analyte appears to be decomposed or unavailable for transport to the torch in a volatile form after this collection process. Nevertheless, these figures provide for an order of magnitude assessment of this figure of merit and again serve to highlight the instability of these species and the reason why their generation from batch reactors is not possible.

In contrast to the case of collection of mercury vapor in such a column of water,[20] more than 80% attenuation of the signal occurred for all other elements studied. A minimum sparge gas flow rate of 0.4 L min^{-1} was necessary to efficiently strip the analytes from solution after collection. Fig. 4 illustrates the effect of shear gas flow rate on the steady-state intensity for Pd following passage of the output from a Ryton double-pass spray chamber through a bubbler column of DIW prior to entry into the torch (with make up gas admitted between the bubbler outlet and the torch so as to provide a constant supply of 0.85 L min^{-1} Ar to the plasma). Under these circumstances, the shear gas flow also serves as the sparge gas flow. It should be noted that if solubilization of the analyte species in the DIW did not occur, the rising edge of the signal in both traces would be vertical. If an insufficient sparge gas flow rate is used (i.e., 0.1 L min^{-1}), minimal intensity of the Pd is recovered because of the continuous dissolution of the analyte in the aqueous phase coupled with its on-going decomposition. When the shear (sparge) gas flow rate is increased to 0.5 L min^{-1}, efficient transfer of the analyte out of the solution then occurs, such that when steady-state conditions are achieved, the signal is similar to that reported in Fig. 2(c) (wherein no bubbler is employed). The first peak on the rising edge of the larger signal likely represents rapid evolution of that portion of the analyte that was dissolved (and accumulated) in the aqueous phase during the period of low shear gas flow rate. The falling edge of the signal reflects the cessation of generation with the introduction of a blank wash solution into the nebulizer. A significant conclusion is that exchange of analyte occurs between the gas and aqueous phases but this leads to minimal decomposition over the residence time of the analyte in the solution, consistent with the fact that preconcentration can be achieved, as discussed above.

Table 5 Effect of spray chamber geometry on relative response

| | Intensity ratio[a] | | | | |
| | Ryton spray Chamber | | Glass spray chamber | | |
	A	B	A	B	C
^{65}Cu	2.0	1.3	1.1	0.33	0.45
^{106}Pd	2.0	1.7	1.8	0.45	0.67
^{107}Ag	2.0	1.4	0.79	0.47	0.48
^{197}Au	2.0	1.0	1.6	0.33	0.46
^{195}Pt	2 .0	1.0	0.75	0.15	0.33
^{59}Co	3 .0	2.0	0.41	0.18	0.24
^{60}Ni	2.0	2.4	0.93	0.45	0.50
^{103}Rh	1.5	0.95	0.68	0.26	0.32
^{205}Tl	2.5	1. 6	1.2	0.56	0.40
^{48}Ti	3.0	1.1	0.38	0.35	0.12
^{55}Mn	2.0	1.1	0.39	0.36	0.10
^{193}Ir	3.0	1.5	0.54	0.93	0.30
^{64}Zn	2.5	0.84	0.28	0.32	0.16
^{114}Cd	3.5	2.2	33	26	15
^{115}In	3.0	2.4	50	11	19
^{202}Hg	1.0	0.90	4.0	4.7	3.5
^{208}Pb	2.0	1.1	6.2	5.6	4.9
^{75}As	1.3	1.8	3.3	2.1	2.0
^{78}Se	1.1	1.7	2.8	4.1	2.8
^{121}Sb	1.2	1.4	3.9	2.9	3.1

[a]Relative to response obtained with a Ryton double-pass spray chamber mounted in a horizontal position. A, Double-pass spray chamber mounted in a vertical position; B, single-pass spray chamber mounted in vertical position; C, double-pass spray chamber mounted in horizontal position.

Spray chamber geometry

A series of experiments to determine the effect of the position of the spray chamber (vertical or horizontal) relative to the nebulizer revealed that when a vertical (drain at the bottom) geometry is used, larger signals occur. Data are summarized in Table 5 and clearly show that, when the spray chamber is mounted in a vertical position, the vapor generation efficiency for transition and noble metals is significantly enhanced (2–3-fold) over the case when the spray chamber is in the conventional (nearly) horizontal position. By contrast, no significant difference is noted for the conventional hydride-forming elements. Both the glass and Ryton spray chambers exhibit this effect. A further significant observation is that when a double-pass spray chamber is used, intensities for the transition and noble elements are 2–3-fold higher than when a single-pass chamber is used. Again, by contrast, this change has a small effect on the signals for conventional hydride forming elements (<40%, and typically a decrease in response). It is believed that these effects are a consequence of the two-step nature of the reaction for these transition metals.[20] This model is based on the assumption that the aquo-ion of the analyte is first reduced to the metal atom and that this intermediate is stabilized in the reaction medium by adsorption onto a surface site. Hydrogen atoms generated from the reductant subsequently react with this intermediate to yield the final product, which then desorbs.[20] The larger surface area provided by the presence of the inner tube of the double spray chamber thus serves to enhance the overall reaction. A more general conclusion is that interactions between reactants in the aqueous phase and the spray chamber surfaces are important. The possibility that fresh reductant is available to interact with a large surface of reactive adsorbed metal atoms serves to enhance the efficiency of the second step of the overall reaction. An interesting observation is that signals for all transition and noble metals studied either disappear completely or are significantly suppressed if the glass surface is silanized prior

Table 6 Wash-in times

| | Time/s[a] | | | |
| | Double Pass Ryton Chamber | | Double Pass Glass Chamber | |
	Horizontal	Vertical	Horizontal	Vertical
^{65}Cu	23	24	71	40
^{106}Pd	35	13	88	69
^{107}Ag	25	25	61	46
^{197}Au	29	27	24	48
^{195}Pt	22	15	40	40
^{59}Co	61	54	86	63
^{60}Ni	28	23	79	46
^{103}Rh	15	19	58	53
^{205}Tl	26	34	47	47
^{48}Ti	22	17	13	19
^{55}Mn	28	22	19	27
^{193}Ir	29	16	20	21
^{64}Zn	25	16	17	16
^{114}Cd	17	13	24	38
^{115}In	32	18	88	60
^{202}Hg	45	45	42	37
^{208}Pb	118	8.7	24	25
^{75}As	22	31	32	32
^{78}Se	21	37	56	55
^{121}Sb	23	27	33	40

[a]Wash-in time defined as time required for response to rise from baseline to steady-state intensity.

to use (rinsing with a 1% dimethyldichlorosilane in hexane), further implicating the role of the surface in mediating these reactions.

A comparison of relative signal wash-in times, summarized in Table 6, shows that when the spray chamber is operated in a vertical position, a shorter signal equilibration time (on average) occurs. This may simply be a consequence of the drainage characteristics of the spray chamber, which give rise to a thinner film of liquid on the surface. A vertical geometry inhibits pooling of slowly draining solution, permitting its more rapid removal from the surfaces on which analyte release takes place. Both effects minimize dissolution and decomposition of the gaseous analyte species in the liquid phase.

A flow injection mode (FI) of sample introduction was used to quantitatively characterize response from the volatile metal species. An example is presented in Fig. 5 for Co. In a glass spray chamber, a long wash out time for the signal is evident in the hydrochloric acid medium (also occurring when using nitric acid), suggesting that cobalt chloride may be adsorbed more easily to this surface, with the result that signal generation continues even after admitting a blank solution during the wash out phase. This memory effect is similar to that noted earlier for Ag (Fig. 2(b)). When using a Ryton spray chamber, the shape of the Co signal is sharp and symmetrical, implying that the generation process is a rapid reaction. Table 7 summarizes data characterizing the full width at half maximum intensity (FWHM) for transient response arising from the introduction of 80 μL volumes of sample into a system fitted with either a Ryton or a glass spray chamber. With FI, signal shape is ideally determined by the dispersion of the plug of analyte in the flowing acid stream used to conduct it to the nebulizer merge point. All signals should, to a first approximation, consequently possess identical transient response characteristics. It is clear, however, that the resulting signal shapes are actually determined by the convolution of the above physical effect with those arising from the (chemical) generation/(physical) transport/(chemical) decomposition of the analyte during its partitioning to the gas phase and subsequent
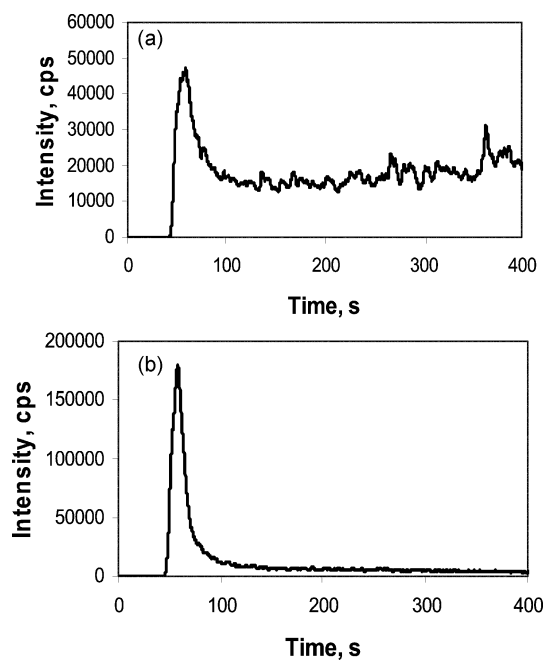
Fig. 5 Flow injection sample introduction of 80 µL of 2 mg L^{-1} Co into a 1.1 mL min^{-1} carrier stream of 0.1 M HCl merging with a 1.1 mL min^{-1} flow of 1% (m/v) NaBH$_4$ solution containing 0.001 M NaOH. (a) With a glass spray chamber; (b) with a Ryton spray chamber.

transport to the plasma. The consequence is that the signal characteristics are entirely dependent on the individual chemical systems. The data in Table 7 that show that the Ryton spray chamber gives rise to narrower and more

Table 7 Flow injection peak parameters[ab]

	FWHM[c]/s		
	Ryton	Glass	Concentration/mg l^{-1}
[65]Cu	16	34 (M)	1
[106]Pd	20	34 (M)	1
[107]Ag	13	21 (M)	0.2
[197]Au	15	47 (M)	0.2
[195]Pt	19	>350 (M)	5
[59]Co	14	26 (M)	2
[60]Ni	14	29 (M)	2
[103]Rh	19	37 (M)	1
[205]Tl	12	17 (M)	0.2
[48]Ti	13	17	1
[55]Mn	14	16	0.5
[193]Ir	14	18	2
[64]Zn	13	16	5
[114]Cd	14	19	0.1
[115]In	12	40 (96)	0.1
[202]Hg	ND	16	0.1
[208]Pb	13	28 (71)	0.1
[75]As	14	19	0.01
[78]Se	12	13	0.05
[121]Sb	15	19	0.01

[a]0.08 mL sample injection volume. [b]ND: not determined. [c]Full width at half maximum signal intensity. Data in parentheses delineate presence of a significant tailing memory effect: $M = >350$ s washout time, defined as time required for signal to decay to 5% of peak intensity.

intense peaks than the glass system for the transition and noble metals.

Conclusion

The vapor generation characteristics of a number of transition and noble metals confirm that the resulting species are relatively unstable in solution and are quickly lost during their generation and subsequent transport, requiring rapid phase separation for efficient detection. The characteristics of the material of the generator and gas–liquid separator significantly affect the signal intensity, as well as its shape. These observations provide support for a two-step model of vapor generation, wherein the wetted surfaces in the system play an intimate role in stabilizing a reduced intermediate of the element.

Acknowledgements

References

1 R. E. Sturgeon, J. Liu, V. J. Boyko and V. T. Luong, *Anal. Chem.*, 1996, **68**, 1883–1887.
2 A. S. Luna, R. E. Sturgeon and R. C. de Campos, *Anal. Chem.*, 2000, **72**, 3523–3531.
3 H. Matusiewicz, M. Kopras and R. E. Sturgeon, *Analyst*, 1997, **122**, 331–336.
4 Y.-L. Feng, J. W. Lam and R. E. Sturgeon, *Analyst*, 2001, **126**, 1833–1837.
5 N. Panichev and R. E. Sturgeon, *Anal. Chem.*, 1998, **70**, 1670–1676.
6 G.-H. Tao and R. E. Sturgeon, *Spectrochim. Acta, Part B*, 1999, **54**, 481–490.
7 C. Moor, J. W. H. Lam and R. E. Sturgeon, *J. Anal. At. Spectrom.*, 2000, **15**, 143–150.
8 A. Sanz-Medel, M. C. Valdes-Hevia y Temprano, N. Bordel Garcia and M. R. Fernandez de la Campa, *Anal. Chem.*, 1995, **67**, 2216–2223.
9 M. L. Garrido, R. Munoz-Olivas and C. Camara, *J. Anal. At. Spectrom.*, 1998, **13**, 295–300.
10 P. Pohl and W. Zyrnicki, *Anal. Chim. Acta*, 2001, **429**, 135–143.
11 P. Pohl and W. Zyrnicki, *J. Anal. At. Spectrom.*, 2001, **16**, 1442–1445.
12 P. Pohl and W. Zyrnicki, *J. Anal. At. Spectrom.*, 2002, **17**, 746–749.
13 X. Duan, R. L. McLaughlin, I. D. Brindle and A. Conn, *J. Anal. At. Spectrom.*, 2002, **17**, 227–231.
14 Y.-K. Lu, H.-W. Sun, C-G. Yuan and X.-P. Yan, *Anal. Chem.*, 2002, **74**, 1525–1529.
15 T.-J. Hwang and S.-J. Jiang, *J. Anal. At. Spectrom.*, 1997, **12**, 579–584.
16 X.-D. Xia, Z.-X. Zhuang, B. Chen and X.-R. Wang, *Analyst*, 1998, **123**, 627–632.
17 C. Vargas-Razo and J. F. Tyson, *Fresenius' J. Anal. Chem.*, 2000, **366**, 182–190.
18 T. Matousek, J. Dedina and M. Vobecky, *J. Anal. At. Spectrom.*, 2002, **17**, 52–56.
19 X. Du and S. Xu, *Fresenius' J. Anal. Chem.*, 2001, **370**, 1065–1070.
20 Y.-L. Feng, R. E. Sturgeon and J. W. Lam, *Anal. Chem.*, 2002, **75**, 635–640.
21 W. W. Ding and R. E. Sturgeon, *Anal. Chem.*, 1997, **69**, 527–531.
22 T. Matousek and R. E. Sturgeon, *J. Anal. At. Spectrom.*, 2003, **18**, 487–494.